



**HAL**  
open science

# Comparison Study of a Second-Generation and of a Third-Generation Wave Prediction Model in the Context of the SEMAPHORE Experiment

Béatrice Fradon, Danièle Hauser, Jean-Michel Lefèvre

► **To cite this version:**

Béatrice Fradon, Danièle Hauser, Jean-Michel Lefèvre. Comparison Study of a Second-Generation and of a Third-Generation Wave Prediction Model in the Context of the SEMAPHORE Experiment. *Journal of Atmospheric and Oceanic Technology*, American Meteorological Society, 2000, 17 (2), pp.197 - 214. 10.1175/1520-0426(2000)0172.0.CO;2 . insu-01646982

**HAL Id: insu-01646982**

**<https://hal-insu.archives-ouvertes.fr/insu-01646982>**

Submitted on 8 Feb 2021

**HAL** is a multi-disciplinary open access archive for the deposit and dissemination of scientific research documents, whether they are published or not. The documents may come from teaching and research institutions in France or abroad, or from public or private research centers.

L'archive ouverte pluridisciplinaire **HAL**, est destinée au dépôt et à la diffusion de documents scientifiques de niveau recherche, publiés ou non, émanant des établissements d'enseignement et de recherche français ou étrangers, des laboratoires publics ou privés.



evolution, some reference spectra were defined, as the Phillips spectrum (Phillips 1977), the Pierson–Moskowitz spectrum (Pierson and Moskowitz 1964), the JONSWAP spectrum (Hasselmann et al. 1973), and the Donelan spectrum (Donelan et al. 1985).

The development of the numerical wave prediction models followed the improvements in the knowledge of the processes involved in the wave evolution. The first-generation models were very simple and did not take into account the nonlinear interactions or did so very simply. The second-generation models did take them into account but only through parameterizations. In the third-generation models, an explicit source term for the nonlinear interactions is included, using the method developed by Hasselmann et al. (1985). So, second-generation models should be more accurate than first-generation ones, and third-generation models should be the most accurate. Although third-generation wave models have a better representation of the physics, it has not been demonstrated that second-generation wave models are inadequate for operational applications, particularly since computational efficiency is important here (Holt 1994).

The implementation of a new model, and in particular of a third generation, requires more personnel and computation resources. Moreover, the increasing availability of satellite data motivates the development of techniques of data assimilation in wave models. The use of the most efficient ones requires a large number of model integrations. The question then arises in the interest of implementing an assimilation scheme in a third-generation wave model for operational forecast, rather than in a second-generation model.

Consequently, the purpose of this study is to attempt to better answer this question, taking advantage of a large dataset from an experiment. Two models were used: the second-generation VAG used at Météo-France (Guillaume 1990) and the third-generation Wave Model (WAM) used at the European Centre for Medium-Range Weather Forecasts (ECMWF) (WAMDI Group 1988). The purpose was to compare the models outputs with each other and with observations. The aim was also to propose possible improvements for VAG. The period chosen for this study corresponds to the one of the SEMAPHORE experiments, which took place in the North Atlantic (between Madeira and the Azores) in October–November 1993 (Eymard et al. 1996). From this experiment both wind and wave measurements were obtained and used in the present study. Moreover, wind and wave data from satellite measurements (TOPEX/Poseidon, *ERS-1*) have been used in this study in order to extend the possibility of comparisons between model outputs and observations.

Section 2 presents VAG and WAM and some basic tests. Section 3 gives a brief description of the SEMAPHORE experiment and of the wind fields and observations used in this study. Section 4 presents the results of hindcasts made with VAG and WAM during

the period of the SEMAPHORE experiment. Sections 5 and 6 give the modification made to improve VAG and the results of the hindcasts made with this new version of VAG. Finally, section 7 gives a summary of this study.

## 2. General characteristics of the VAG and WAM models

Both models used in the present study were developed to be used on operational basis. VAG is a second-generation wave prediction model developed in the 1980s at Météo-France (Guillaume 1990). WAM is a third-generation wave prediction model developed in 1988 at ECMWF (WAMDI Group 1988).

Both models are based on the solution of the equation for the conservation of action (Phillips 1977). The following sections (2a–2b) give more details about these models, and Table 1 presents the configuration of the models used in the present study.

### a. The VAG model

The operational version of VAG is run on a polar stereographic grid on the North Atlantic Ocean, assuming deep water at each grid point.

The VAG version used in the study presented here uses a spherical  $0.5^\circ$  grid. The second-order advection scheme implemented in the operational version was replaced here by a first-order scheme, which tends to smooth the garden sprinkler effect. This version will soon become operational. It will simply be referred to as VAG in the following.

Under the deep water assumption and without current, the equation for the conservation of wave action can be simplified to obtain the following equation for the evolution of the wave spectrum  $F(f, \theta)$ :

$$\begin{aligned} \frac{\partial F(f, \theta)}{\partial t} + \mathbf{c}_g \cdot \nabla F(f, \theta) + \frac{\partial}{\partial \theta} [(\mathbf{c}_g \cdot \nabla \theta) F(f, \theta)] \\ = S(f, \theta), \end{aligned} \quad (1)$$

where  $f$  and  $\theta$  the wave frequency and propagation direction, respectively;  $\mathbf{c}_g$  their group velocity; and  $S$  the source/sink term.

The physical part of the model is identical to the one used in the operational version of VAG: the source/sink term  $S(f, \theta)$  consists of a linear growth term,  $S_{\text{lin}}$ , representing the Phillips' growth process (Phillips 1957); an exponential growth term,  $S_{\text{exp}}$ , representing the Miles' growth (Miles 1957); and a dissipation term,  $S_{\text{dis}}$ , representing dissipation due to wave breaking as given by Golding (1983). The expressions for these source or sink terms are detailed in the appendix.

The effects of the nonlinear interactions are taken into account in an indirect way that consists of two steps. In the first step, the region of the wave spectrum that corresponds to the wind–sea is delimited and the total

TABLE 1. Configuration for VAG and WAM in the present study.

	Configuration of VAG in the present study	Configuration of WAM in the present study	Modified version of VAG in the present study
Water depth assumption	Deep water	Deep water	Deep water
Spatial discretization	Spherical grid, $0.5^\circ \times 0.5^\circ$	Spherical grid $0.5^\circ \times 0.5^\circ$	Spherical grid, $0.5^\circ \times 0.5^\circ$
Spatial domain	( $10^\circ$ – $70^\circ$ N), ( $80^\circ$ W– $10^\circ$ E)	( $10^\circ$ – $70^\circ$ N), ( $80^\circ$ W– $10^\circ$ E)	( $10^\circ$ – $70^\circ$ N), ( $80^\circ$ W– $10^\circ$ E)
Numerical scheme	Advection: first-order upstream Source term: explicit scheme	Advection: first-order upstream Source term: implicit scheme	Advection: first-order upstream Source term: explicit scheme
Time step	15 min	15 min	15 min
Number of frequency bands/ frequency range	22, geometric progression 0.040–0.296 Hz	25, geometric progression 0.0418–0.412 Hz	22, geometric progression 0.040–0.296 Hz
Number of direction bands	18	18	18
Growth term	Linear (Golding 1983) + exponential (Snyder et al. 1981)	Exponential (Janssen 1991) but without the wind–wave coupling	Exponential (Janssen 1991) but without the wind–wave coupling
Dissipation term	Golding 1983	Hasselmann (1974) modified	Hasselmann (1974) modified
Nonlinear interaction term	Not explicit	Hasselmann et al. 1985	Not explicit

energy of this domain is limited if necessary by the total energy of the Pierson–Moskowitz spectrum (Pierson and Moskowitz 1964) corresponding to the fully developed spectrum associated with the specified wind speed. This is the “limitation of the wind–sea energy,” which aims to avoid imbalances between growth and decay. In the second step of calculation, the wind–sea part of the spectrum is reshaped into a JONSWAP spectrum (Hasselmann et al. 1973) with a  $\cos^2$  distribution on each side of the wind direction. This is the “redistribution of the wind–sea energy.” The configuration (resolution, domain, etc.) as used in the present study is given in Table 1.

### b. The WAM model

The WAM source codes offers a range of possibilities (deep or shallow water, spherical or stereographic grid, etc.) but in this study we chose to make VAG and WAM be as close as possible (see Table 1). So WAM was used in a deep water mode on the same spherical grid as VAG and with the same first-order propagation scheme. However, the physical part of the WAM model differs quite appreciably from the VAG part. There is no linear growth term in WAM (the spectrum is initialized with a low-energy JONSWAP spectrum) and WAM exponential growth and dissipation terms differ from those of VAG (see the appendix for the detailed expressions used in WAM). More importantly, the main difference is that WAM includes an explicit source term for the nonlinear interactions. For the present study, WAM has been run in two versions. In the first one, the wind–wave coupling term proposed by Janssen (1991) has been kept as in the original code of WAM cycle 4. In the second case, the wind–wave coupling term has been removed (see the appendix), keeping all coefficients similar to the first version. We mainly focus on the

results obtained with this second version because its configuration is closer to that of VAG. Results obtained with the complete cycle 4 version are mentioned when necessary.

### c. Growth curves

A first step in this study was the comparison of the growth and decay curves obtained with VAG and WAM. These curves were obtained by running a “one-point” version (without advection) of each model forced by a wind constant during 48 h (two wind speed cases were studied: 18.25 and 6.75  $\text{m s}^{-1}$ ). After 48 h, the wind speed is abruptly changed to 0.25  $\text{m s}^{-1}$  and kept to this constant value for the next hours of the simulation. The configuration of this simulation is close (although not exactly identical) to the one discussed by Günther et al. (1992) and Komen et al. (1994). The wind speed value could not be chosen exactly identical because VAG uses precalculated terms based on a discretization of wind speeds every 0.5  $\text{m s}^{-1}$ .

The time series of the significant wave height (SWH) is plotted in Fig. 1 for VAG and Fig. 2 for WAM (upper plots). Figures 1 and 2 also show in the bottom plots the temporal evolution of the different terms of the energy budget (integrated over each time step of 15 min): linear and exponential growth, dissipation, energy limitation, and nonlinear interactions. In the case of VAG, this latter term is zero because the reshaping of the wind–sea part of the spectrum is energy conservative. The “limitation term” corresponds to the energy that is removed at each time step from the energy budget after growth and dissipation has taken place. For VAG, this term corresponds to the difference between the energy of the wind–sea part found after growth and dissipation and the energy of a Pierson–Moskowitz spectrum. This limitation is introduced into the physical











TABLE 2. Statistics of collocated datasets of reanalyzed ARPEGE wind speeds and ECMWF wind speeds with satellite measurements. Mean differences and standard deviations are in meters per second. The collocated datasets contain 15 632 collocated points for TOPEX/Poseidon and 12 398 points for *ERS-1*. The mean wind speed and standard deviation are, respectively, 7.25 and 2.68  $\text{m s}^{-1}$  for TOPEX/Poseidon, 7.40 and 3.58  $\text{m s}^{-1}$  for *ERS-1*, 7.13 and 3.54  $\text{m s}^{-1}$  for the reanalyzed ARPEGE winds collocated with TOPEX/Poseidon, 7.47 and 3.58  $\text{m s}^{-1}$  for the ECMWF winds collocated with TOPEX/Poseidon, 7.37 and 3.71  $\text{m s}^{-1}$  for the reanalyzed ARPEGE winds collocated with *ERS-1*, and 7.67 and 3.70  $\text{m s}^{-1}$  for ECMWF winds collocated with *ERS-1*.

	TOPEX/Poseidon			<i>ERS-1</i>		
	Mean difference	Std dev	Correlation	Mean difference	Std dev	Correlation
Reanalyzed						
ARPEGE winds	-0.12	2.19	0.787	-0.03	2.23	0.814
ECMWF winds	0.22	2.06	0.821	0.27	2.02	0.846

provided by the ships and buoys deployed during the campaign and by the *ERS-1* scatterometer (Le Meur et al. 1994). All the available wind data from ships and buoys were used in this reanalysis, even if they would have arrived too late for a real-time analysis. Reanalyzed ARPEGE winds are available for the entire North Atlantic with a  $0.5^\circ$  resolution every 6 h. No wind estimates from satellite altimeter measurements were used for these reanalyses.

The second type of wind fields—hereafter referred to as ECMWF winds—corresponds to the output of the operational atmospheric model used at ECMWF. The wind data provided by the ships and buoys deployed during the campaign were also assimilated in the ECMWF atmospheric model but it was an operational assimilation (only data transmitted in time are taken into account in the assimilation). ECMWF winds are available with a  $1^\circ$  resolution and have been then linearly interpolated on the  $0.5^\circ$  resolution grid of the wave models every 6 h.

The differences between the two wind fields (reanalyzed ARPEGE and ECMWF) may come from (i) the model itself and its associated assimilation method, (ii) the number of standard observations that were assimilated (only data that arrived in time for the real-time analysis have been used for the ECMWF winds), or (iii) the assimilation of *ERS-1* scatterometer data in the case of the reanalyzed ARPEGE winds.

Table 2 shows a comparison of the reanalyzed ARPEGE wind speeds and the ECMWF wind speeds with the observations from the altimeters of the TOPEX/Poseidon and *ERS-1* satellites during October 1993. The mean differences between modeled and observed winds are a few centimeters per second and the standard deviations are of the order of  $2 \text{ m s}^{-1}$ . These results are significant at the 99% confidence level because of the large database available. The mean differences and standard deviations are of the same order of magnitude for both wind fields, which seems to show that both wind fields are of the same quality. However, the correlation between modeled and observed winds is higher for the ECMWF winds. As a consequence, we will focus here on the results obtained when driving the wave models with the ECMWF winds. It should be noted that runs

were also performed by forcing VAG and WAM with the reanalyzed ARPEGE winds in order to study the impact of the winds on the results of the wave models.

#### 4. Comparison between the results of the VAG and of the WAM

Two hindcasts were performed by forcing VAG and WAM by the ECMWF winds during October 1993 on the entire North Atlantic. In this section we compare the results of these two hindcasts.

##### a. General comparison of the SWHs

The analysis of the wave fields for the whole period showed that the structure of the SWH fields is quite similar in both models. Particularly, the positions and shapes of the areas of high SWHs are very close in VAG and WAM. This agreement was confirmed by a statistical comparison between VAG and WAM SWHs at all sea points every 3 h during October 1993 (3 888 144 data for each model): the correlation coefficient obtained is 0.92. However, WAM SWHs are about 13 cm lower than those for VAG (mean SWHs are, respectively, 2.41 and 2.28 m for VAG and WAM). So the variations of the SWHs in both models is similar but with a systematic mean difference between VAG and WAM.

These results are confirmed by a statistical comparison of the SWHs hindcasted by VAG and WAM (with both models forced by the ECMWF winds) with the measurements from TOPEX/Poseidon and *ERS-1*. Satellite observations and models data were collocated, as explained in section 3b. The result of this comparison is summarized in Table 3.

For the hindcasts run with the ECMWF wind fields, and those run with WAM using the version without wind-wave coupling, the mean differences between the models' SWHs and those of the satellites are small and of the same order of magnitude for both models (0.07 to 0.08 m for VAG;  $-0.06$  to  $-0.11$  m for WAM). However, when WAM is used in its complete cycle 4 version (with the wind-wave coupling) a significant negative bias is found with respect to the satellite data





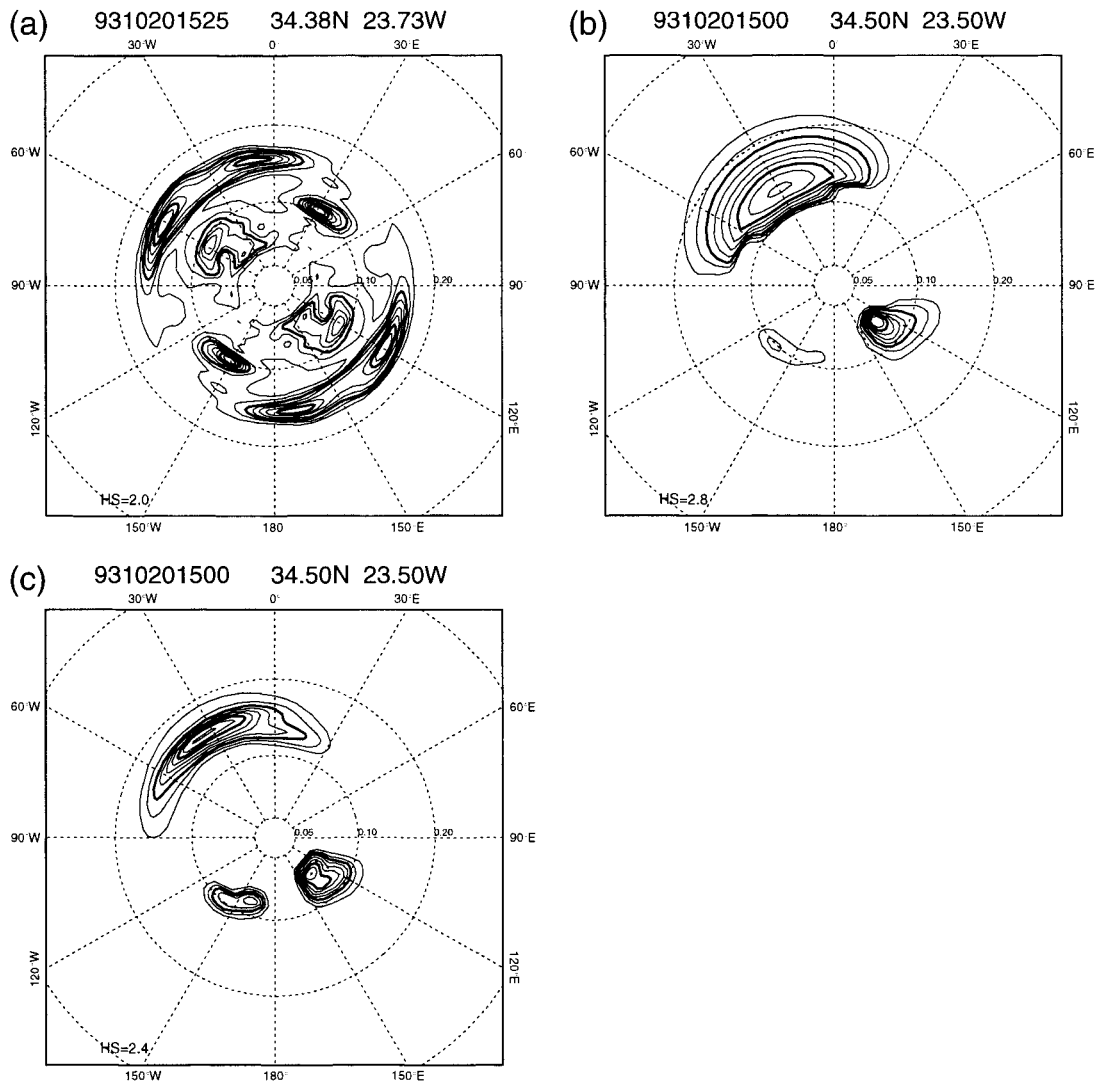


FIG. 9. (a) Directional spectrum of the waves measured with the airborne radar RESSAC on 20 Oct at 1525 UTC and corresponding spectra obtained with (b) VAG and (c) WAM. The spectra are normalized and the isolines are plotted from 0.1 to 0.9 every 0.1. The distance to the center of the plot is proportional to the frequency of the waves. The SWH is given at the bottom of each spectrum. Note that the RESSAC data are obtained with a 180° ambiguity in the propagation direction that was not removed in the figure.

Moreover, a statistical comparison of the SWHs hind-casted by VAG and WAM with the satellites measurements (section 4) showed that the WAM SWHs were better correlated with the TOPEX/Poseidon and *ERS-1* data, although they presented a significant mean difference. So we tried to remedy these weaknesses of VAG by testing some modifications.

The study of VAG and WAM growth and decay curves showed that the energy balance in the VAG model was not very satisfactory (section 2). Two main weaknesses of VAG were evidenced. First, the linear growth term was too high, whereas the exponential growth term and the dissipation term were too low compared to WAM. Second, the energy input due to the wind and the energy output due to the breaking of the waves were

not well balanced. So, a limitation of the wind–sea energy was shown to be necessary, but it was quite large and resulted in losses of energy (see sections 2c–d and Figs. 1 and 3).

In order to improve the behavior of the VAG model, we tried to make VAG have a better balance between growth and decay. This was performed by replacing the exponential growth and dissipation terms used in VAG by the ones used in WAM. Because of the differences between VAG and WAM, this could not be done without readjusting VAG, which was made by taking into account weighting coefficients for the linear growth, the exponential growth, and the dissipation. These coefficients were chosen so that the growth and decay curves of the modified VAG version were in overall good











- , 1977: *The Dynamics of the Upper Ocean*. 2d ed. Cambridge University Press, 336 pp.
- , 1985: Spectral and statistical properties of the equilibrium range in wind-generated gravity waves. *J. Fluid Mech.*, **156**, 506–531.
- Pierson, W. J., and L. Moskowitz, 1964: A proposed spectral form for fully developed wind sea based on the similarity theory of S. A. Kitaigorodskii. *J. Geophys. Res.*, **69**, 5181–5190.
- Snyder, R. L., F. W. Dobson, J. A. Elliott, and R. B. Long, 1981: Array measurements of atmospheric pressure fluctuations above surface gravity waves. *J. Fluid Mech.*, **102**, 1–59.
- Tournadre, J., B. Chapron, and R. Abdellaoui, 1994: Données spatiales, partie 1: Données de vent et de vagues. *SEMAPHORE Rep. 6*, IFREMER, 80 pp. [Available from J. Tournadre, IFREMER, BP 70, 29280 Plouzané Cedex, France.]
- van Vledder, G. P., and L. H. Holthuijsen, 1993: The directional response of ocean waves to turning winds. *J. Phys. Oceanogr.*, **23**, 177–192.
- WAMDI Group, 1988: The WAM Model—A third-generation ocean wave prediction model. *J. Phys. Oceanogr.*, **18**, 1775–1810.
- WMO 1989: Guide to wave analysis and forecasting. WMO Rep. 702, 233 pp. [Available from WMO, 7 bis avenue de la Paix, CP 2300, 1211 Geneva 2, Switzerland.]
- Wu, 1982: Wind-stress coefficients over sea surface from breeze to hurricane. *J. Geophys. Res.*, **87**, 9704–9706.
- Young, I. R., S. Hasselmann, and K. Hasselmann, 1987: Computations of the response of a wave spectrum to a sudden change in wind direction. *J. Phys. Oceanogr.*, **17**, 1317–1338.